Space Radiation Dose Rates in the Earth's Atmosphere

J. W. HAFFNER*
North American Aviation, Downey, Calif.

This paper presents a calculation of nuclear radiation dose rates within the earth's atmosphere due to natural space radiation. Two conditions are considered—active sun and quiet sun. The active sun environment includes depressed galactic (cosmic) radiation fluxes and solar flare radiation based upon a model similiar to the Bailey model event. The quiet sun environment includes only the nondepressed galactic radiation. The spectra for both environments were truncated at the geomagnetic cutoff energy for the undisturbed field. Atmospheric attenuation was taken into account by using simple range-energy relations. Asymptotic nuclear reaction cross sections were used to calculate cascade and evaporation secondary fluxes. Gibson's flux-to-rad-dose conversion function and Rossi's RBE-LET relationship were used to yield rad and rem dose rates. In this way, dose rates as a function of altitude (10,000–100,000 ft) and geomagnetic latitude (0–90°) for both active and quiet sun conditions were obtained. The significance of the dose rates obtained for passengers and crew members of the Supersonic Transport (SST) is discussed.

Introduction

THE natural nuclear radiations present in the earth's atmosphere constitute one of the environments in which present and future aircraft must operate. As the altitudes at which aircraft operate increase, the importance of this environment also increases. For high-altitude flights over the earth's polar regions, the nuclear radiation environment may become sufficiently severe under certain conditions to require modification of the flight mission profile. For many aircraft, modifying the flight profile is undesirable for reasons of economy, national defense, or safety. Therefore, it is important that the nuclear radiation environment be sufficiently well understood so that the flight profile will not be altered on its account unless absolutely necessary.

Several prior studies of the role of nuclear radiations in space on high-flying aircraft and their occupants have been carried out. Among the more significant are studies pertaining to the Supersonic Transport (SST) by Schaefer,[1] Dye and Sheldon,[2] Shen,[3] Mohler,[4] Foelsche,[5] and a recent one by Nold, Adams, and Supko.[6] However, detailed calculations of rad and rem dose rates as functions of position have not been published. The purpose of the present study was to calculate such dose rates so that the biological effects upon aircraft passengers could be more accurately assessed.

Space Radiation Environment

The principal sources of nuclear space radiation in the earth's atmosphere are solar flare radiation and galactic (cosmic) radiation. The Van Allen belts, which are apparently populated by solar and galactic radiations, are unimportant below ~100 miles altitude, even in the South Atlantic anomoly. The solar wind does not penetrate the geomagnetosphere (~8–12 earth radii distant) except possibly when the field becomes sufficiently distorted to permit them to precipitate at the poles. Even under these conditions, the ranges of solar wind particles are so short that they will not contribute to the dose rates inside aircraft. Therefore, only solar flare and galactic radiations are considered here.

Solar flare nuclear radiation has been studied extensively since 1946 when Forbush[7] first showed that the sun was the source of high-energy charged particles. Since then, over 80 flares have been observed which produced particulate radiation at the earth. Tabulations of these events and their characteristics have been published by Webber,[8] McDonald,[9] Lewis et al.,[10] and others. Galactic (cosmic) radiation was discovered in 1911 by V. F. Hess as the source of exterrestrial ionization.[11] Since then, the characteristics of this radiation have been extensively investigated, especially those concerned with interactions in the atmosphere. Several books dealing with galactic (cosmic) rays have been written.

Solar flares are optical phenomena that are observed to take place in the solar atmosphere. Associated with this optical radiation, the sun is observed to emit other types of radiation (see Fig. 1).[12] Large flares are believed to result in the ejection of a large plasma cloud that may expand to several solar diameters by the time it reaches 1 AU (astronomical unit = 93,000,000 miles). If the earth lies in the path of this plasma cloud, the cloud passes around the geomagnetosphere, compressing and disturbing it somewhat. During the time the plasma cloud envelopes the earth, several effects are observed (see Fig. 1). The effects of interest here are nuclear radiation and rf (radio frequency) blackout. Solar flare occurance probabilities appear to follow the ~11-yr sunspot-number cycle, lagging approximately a year behind it. The recent solar flare radiation history on an annual basis is presented in Table 1.[8] Preliminary estimates are that solar flare radiation occurance probabilities vary an order of magnitude or more from solar maximum (1959–1960) to solar minimum (1965).

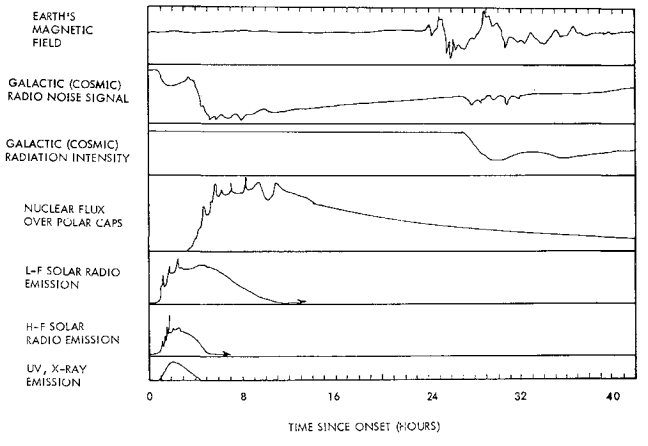

Fig. 1 Sequence of events accompanying a solar flare event as observed from earth.

Presented as Preprint 65-511 at the AIAA Second Annual Meeting, San Francisco, Calif., July 26–29, 1965; submitted July 29, 1965; revision received September 12, 1966.

* Research Scientist, Space and Information Systems Division. Member AIAA.

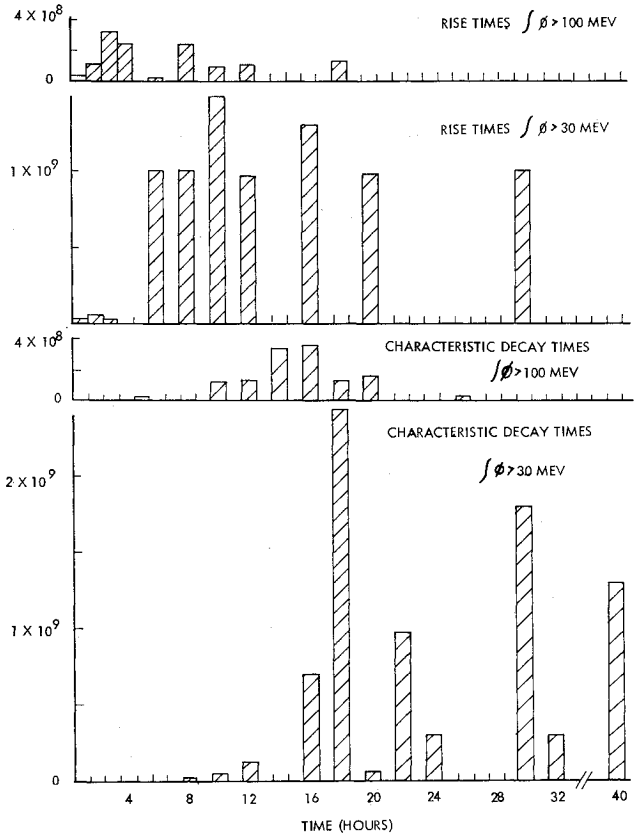

Fig. 2 Size-weighted distributions of rise and decay times for solar flare protons observed at earth.

The parameters of the solar flare nuclear radiations detected at the earth are difficult to correlate with observable parameters. The peak ($\hat{\phi}$ in protons/cm²-sec) and total ($\int\phi$ in protons/cm²) proton and alpha particle fluxes for the nine largest observed flare events are listed in Table 2. In addition, the particle flux rates are specified by onset plus rise times and characteristic decay times as functions of energy.[9] The onset plus rise time (hereafter called the rise time) is the interval between the observation of the peak of the optical radiation from the sun and the peak of the particle fluxes at the earth. The characteristic decay time is the interval required for the peak particle flux rate to decrease a factor of e. The size-weighted values of the rise and decay times for solar flare protons observed since 1956 are shown in Fig. 2.[13] Combining this data with that presented in Table

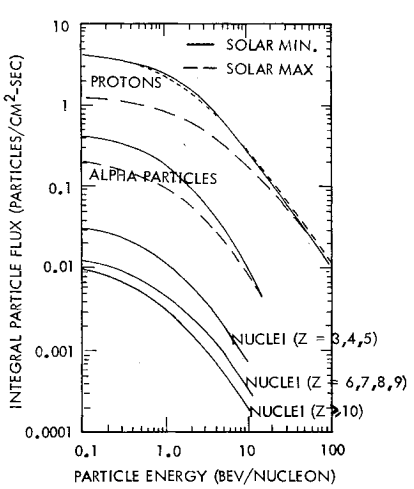

Fig. 3 Integral energy spectra of the various components of the primary galactic (cosmic) radiation.

1 yields the following energy-time dependence of the proton integral energy spectra observed near the earth:

$$\phi(E > E_0, t) = \frac{Ate^{-\alpha E_0^n t}}{E_0^m} \quad (1)$$

where

$\phi(E > E_0, t)$ = proton flux (protons/cm²-hr) above an energy E_0
E = proton energy (Mev)
t = time (hr)
α = 0.022 } constants for large events
m = 0.75 } constants for large events
n = 0.4 } constants for large events
A = normalization factor for the event
= $\sim 10^{\gamma-1}$ for a 10^γ event (10^γ protons/cm² >30 Mev)

Equation (1) is qualitatively quite similar to the time-energy history of the Bailey Model Event.[14]

From Equation (1), the following expressions can be derived:

$$\int\phi(E > E_0) = \frac{A}{\alpha^2 E_0^{m+2n}} \text{ (protons/cm}^2\text{)}$$

$$\hat{\phi}(E > E_0) = \frac{a\, e^{-1}}{\alpha\, E_0^{m+n}} \text{ (protons/cm}^2\text{-hr)}$$

where

$\int\phi(E > E_0)$ = total flux above energy E_0 integrated from time $t = 0$ to $t = \infty$
$\hat{\phi}(E > E_0)$ = peak flux rate of the integral energy spectrum above E_0, which occurs at $t = 1/\alpha E_0 n$ (hr)

Since all particles above the energy threshold (which is a function of altitude and geomagnetic latitude) will be able to reach the point in question, the worst case occurs when the energy integral flux is a maximum. This occurs at $t = 1/\alpha E_0 n$ hr, and the corresponding differential energy spectrum at this time is

$$\phi(E)dE = \frac{A(m+n)e^{-1}}{\alpha E^{m+n+1}} dE \text{ (protons/cm}^2\text{-hr-Mev)}$$

For the envelope of the largest observed flare events (see Table 1), $A \sim 1.5 \times 10^8$. Therefore, the peak differential energy spectrum for this case is

$$\hat{\phi}(E)dE = (2.9 \times 10^9/E^{2.15})dE \text{ (protons/cm}^2\text{-hr-Mev)} \quad (2)$$

This expression was used as the maximum solar flare proton spectrum that would be expected if no shielding mechanisms were present. Tables 1 and 2 also show that on an energy/particle basis (as contrasted to an energy/nucleon basis), an average of 0.8 alpha particles are emitted for each proton.[15] It is postulated that this ratio is a constant throughout the flare radiation event. The role of these alpha particles is

Table 1 Annual history of solar flare proton fluxes observed near the earth[a]

Year	$\int\phi > 10$ mev	$\int\phi > 30$ mev	$\int\phi > 100$ mev
1956	2.6×10^9	1.1×10^9	3.7×10^8
1957	1.0×10^{10}	8.5×10^8	5.9×10^7
1958	9.5×10^9	1.3×10^9	9.5×10^7
1959	2.2×10^{10}	4.2×10^9	4.2×10^8
1960	7.0×10^9	2.1×10^9	3.9×10^8
1961	2.1×10^9	4.1×10^8	5.0×10^7

[a] Fluxes are in units of protons/cm²-yr.

Table 2 Peak ($\hat{\phi}$) and total ($\int \phi$) proton (top number) and alpha particle (bottom number) fluxes observed for nine large flares[a]

Date	$\hat{\phi} > E_0$ (particles/cm²-sec)			$\int\phi > E_0$ (particles/cm²)		
	$E_0 = 10$	$E_0 = 30$	$E_0 = 100$	$E_0 = 10$	$E_0 = 30$	$E_0 = 100$
2-23-56	1.0×10^4 (?)	8.0×10^3 (?)	5.0×10^3 (?)	1.8×10^9 (?)	1.0×10^9 (?)	3.5×10^8 (?)
3-23-58	8.0×10^3 (42)	1.2×10^3 (60)	1.0×10^2 (1.2)	2.0×10^9 (8.5×10^7)	2.5×10^8 (7×10^6)	1.0×10^7 (8×10^4)
8-26-58	1.5×10^4 (?)	1.5×10^3 (?)	5×10^1 (?)	1.5×10^9 (?)	1.1×10^8 (?)	2.0×10^6 (?)
5-10-59	3.0×10^4 (5000)	6×10^3 (500)	1×10^3 (5)	5.5×10^9 (7.5×10^8)	9.6×10^8 (4.2×10^7)	8.5×10^7 (3.5×10^5)
7-10-59	1.5×10^4 (800)	4×10^3 (160)	1.2×10^3 (5)	4.5×10^9 (1.6×10^8)	1.0×10^9 (2.4×10^7)	1.4×10^8 (5×10^5)
7-14-59	5.0×10^4 (10000)	1.0×10^4 (1000)	1.2×10^3 (10)	7.5×10^9 (1.3×10^9)	1.3×10^9 (8×10^7)	1.0×10^8 (7×10^5)
7-16-59	1.0×10^4 (5,000)	6×10^3 (1500)	1.5×10^3 (100)	3.3×10^9 (7.5×10^8)	9.1×10^8 (1.2×10^8)	1.3×10^8 (6×10^6)
11-12-60	3.2×10^4 (4,000)	1.2×10^4 (1500)	2.5×10^3 (180)	4×10^9 (4×10^8)	1.3×10^9 (1.2×10^8)	2.5×10^8 (1.1×10^7)
11-15-60	2.2×10^4 (4,200)	8.0×10^3 (1500)	2.4×10^3 (160)	2.5×10^9 (3.3×10^8)	7.2×10^8 (9×10^7)	1.2×10^8 (6.5×10^6)

[a] E_0 is in units of Mev/nucleon.

discussed in some detail in the "Shielding" section of this paper.

Galactic (cosmic) radiation outside the geomagnetosphere consists of an essentially isotropic flux of bare nuclei having approximately the same atomic number distribution as matter in our galaxy (see Table 3).[12] The particle fluxes are low but the particle energies are very high. The measured integral energy spectra for this galactic radiation are shown in Fig. 3. As can be seen, solar flare activity reduces the galactic radiation fluxes, especially for the low energy ($\lesssim$1 Bev) portion of the spectra. This phenomenon (the Forbush effect) is due to the magnetic shielding the solar flare plasma provides as it envelopes the earth.

The galactic proton and alpha particle integral energy spectra for solar minimum conditions may be fit by the expression[16]

$$\phi(E > E_0) = a/(B + E_0^{1.5}) \text{ particles/cm}^2\text{-sec} \qquad (3)$$

where

$\phi(E > E_0)$ = flux of particles above energy E_0 (Bev)
E = particle energy (Bev)
a = 20 for protons, 2 for alpha particles } constants
B = 5 } constants

The energy derivative of Eq. (3) is

$$\phi(E)\, dE = \frac{1.5\, a\, (E)^{0.5}}{[B + E^{1.5}]^2}\, dE \text{ (particles/cm}^2\text{-sec-Bev)}$$

Table 3 Composition of nuclei present in galactic (cosmic) radiation

Element	Relative abundance in galactic (cosmic) radiation	Relative abundance in universal composition
Hydrogen ($Z = 1$)	100,000	100,000
Helium ($Z = 2$)	10,000–15,000	7,700–10,00
Light nuclei ($Z = 3, 4, 5$)	100–240	0.1
Medium nuclei ($Z = 6, 7, 8, 9$)	500–1200	300
Heavy nuclei ($10 \leqslant Z \leqslant 30$)	200	100
Very heavy nuclei	10–4	10^{-6}

Converting this to more conventional units yields

$$\phi(E)\, dE = \frac{3.5 \times 10^9\, (E)^{0.5}}{[1.6 \times 10^5 + E^{1.5}]^2}\, dE \text{ (protons/cm}^2\text{-sec-Mev)} \qquad (4)$$

where E is in Mev. Equations (2) and (4) were used in the calculation of dose rates in the atmosphere.

Shielding

Two mechanisms act to limit the solar flare and galactic radiation arriving at any point within the earth's atmosphere. The first is the geomagnetic field that deflects charged particles not arriving along the earth's magnetic axis. The result is that there is a minimum momentum/unit charge that a particle must possess if it is to reach any given altitude and latitude (see Fig. 4).[17] Particles arriving at any point in question still possess (in the absence of the atmosphere) their original energy, however. The flux of such particles is only a fraction of the total that would otherwise be able to reach the point in question.

The second mechanism that acts to limit the radiation arriving at any point in the atmosphere is the atmosphere itself. The protons and alpha particles that constitute the primary space radiations lose energy by ionization in the atmosphere. The energy required for a primary particle to reach any par-

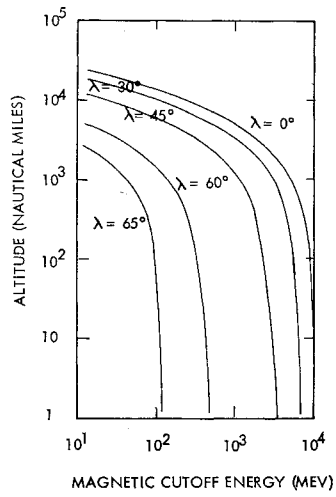

Fig. 4 Geomagnetic cutoff energies for protons as a function of altitude and geomagnetic latitude.

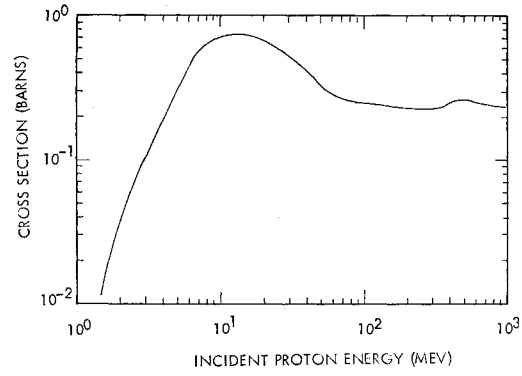

Fig. 5 Nonelastic cross section for protons in air (80% nitrogen, 20% oxygen).

ticular altitude in the atmosphere[18,19] is given by range-energy relations. Notice that Fig. 4 assumes a magnetic field but no atmosphere, whereas the range-energy relation is based on the converse assumptions. At any altitude and latitude, the actual energy spectrum is the result of the effects of both factors.

The attenuation of nuclear space radiation in the atmosphere is due to two mechanisms—atomic ionization and nuclear reactions. At low energies ($\lesssim$ 200 Mev) atomic ionization predominates. In this energy region, the distance (range) a heavy charged particle will travel is a definite function of its energy, with only small variations because of statistical variations (straggling). Therefore, range-energy relationships are meaningful and can be used.

The range-energy relationship for heavy charged particles may be fit by the expression

$$R = \delta E^{\beta} \tag{5}$$

where

R = particle range (g/cm^2)
E = particle energy (Mev)
δ = 2.39×10^{-3} (protons) } for air
= 2.04×10^{-4} (alpha particles) }
β = 1.777 (protons and alpha particles) }

Equation (5) leads to the relationship

$$E' = [E_0^{\beta} - (X/\delta)]^{1/\beta} \tag{6}$$

where

E_0 = incident particle energy (Mev)
E' = emergent particle energy (Mev)
X = shield thickness (g/cm^2)

Equation (6) gives the relation between incident and final energies so long as atomic ionization processes predominate. This is generally true for values of $X \lesssim 30$ g/cm^2. For the attenuation of nuclear space radiation in the earth's atmosphere, this corresponds to an altitude of ~80,000 ft. Below this altitude, nuclear interactions become increasingly important.

Nuclear reactions will produce secondary particles in the atmosphere. For protons, these secondary particles are cascade productions (emitted in $\sim 10^{-20}$ sec) and evaporation nucleons (emitted in $\sim 10^{-15}$ sec). Although both time estimates are only illustrative, the cascade products are chiefly nucleons that are "knocked out" of the target nucleus by the incident proton, whereas the evaporation products are "boiled off" the still excited nucleus so long as sufficient energy remains. Beta and/or gamma ray emission accounts for the residual portion of the nuclear energy. Usually some mesons are also produced as part of the cascade process, which in turn produces electrons and gamma rays. Because of the relativistic effects present at such high energies (several hundred

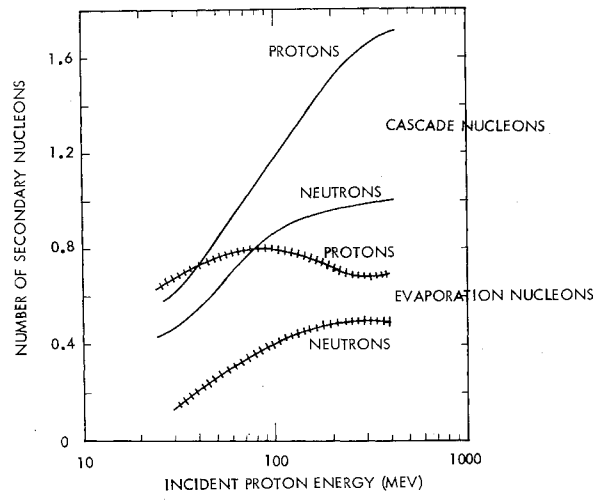

Fig. 6 Number of cascade and evaporation nucleons emitted per nonelastic collision by incident protons in air.

Mev) the cascade products are projected forward in the general direction of the primary particle. These cascade products can produce nuclear reactions of their own, etc. Thus, a "shower" of nuclear particles and radiations is built up. On the other hand, evaporation nucleons and residual nuclear radiations are emitted essentially isotropically.

For protons in air, the nonelastic cross section (see Fig. 5) and nuclear multiplicities[20] (see Fig. 6) are largely based on Bertini's theoretical work.[21,22] The cross section and the nuclear multiplicities becomes essentially constant above a few hundred Mev and were therefore extrapolated. The atmosphere was assumed to have a constant composition of 20% oxygen, 80% nitrogen independent of altitude. Two differences between the atomic ionization and the nuclear reaction attenuation mechanism should be noted. Ionization reduces the energy of each primary particle without affecting the flux of such particles, whereas nuclear reactions produce just the opposite effects. This is a consequence of the deterministic nature (i.e., good statistics) of the atomic ionization attenuation vs the probabilistic nature (i.e., poor statistics) of the nuclear reaction attenuation.

In order to facilitate the calculations, the attenuation of the atmosphere in the absence of the geomagnetic field was investigated. The flux (ϕ) of the primary protons at any atmospheric depth was calculated from the relation

$$\phi = \phi_0 e^{-n\sigma x/\rho} \text{ (protons/cm}^2\text{-hr-Mev)} \tag{7}$$

where

ϕ_0 = incident flux [from Eqs. (2) and (4)]
n = nuclear density in sea level atmosphere (5×10^{19} nuclei/cm^3)

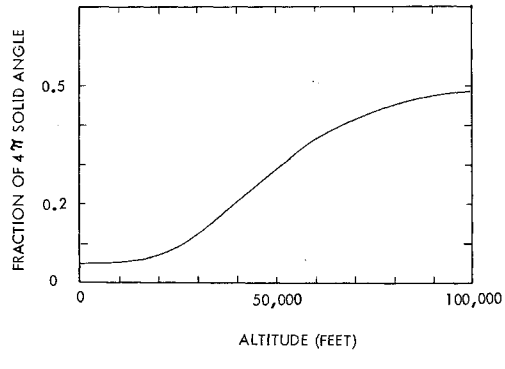

Fig. 7 Effective fraction of 4π solid angle through which nuclear space radiation reaches any altitude in earth's atmosphere.

ρ = sea level atmospheric density (1.2×10^3 g/cm^2)
X = atmospheric depth (g/cm^2)

The surviving primary protons at any atmospheric depth do not possess their incident energy, since ionization losses decrease it according to Eq. (6). In using Eq. (6), it was easiest to integrate Eqs. (2) and (4) over energy from E_0 to ∞, substitute using Eq. (6), and differentiate. Straightforward substitution of Eq. (6) into Eqs. (2) and (4) is incorrect, since the energy increment dE' stretches relative to dE as the final energy E' decreases. Thus Eqs. (2) and (4) become, respectively,

For model flare radiation:

$$\phi(E', x) = \frac{2.9 \times 10^9 (E')^{0.777} e^{-0.01x}}{[(E')^{1.777} + (x/2.39 \times 10^{-3})]^{1.65}} \quad (8)$$

For galactic radiation:

$$\phi(E', X) = \frac{3.59 \times 10^9 (E')^{0.777}\, e^{-0.01x}}{[(E')^{1.777} + (X/2.39 \times 10^{-3})]^{0.15} \times \{1.65 \times 10^5 + [(E')^{1.777} + (x/2.39 \times 10^{-3})]^{0.85}\}^2} \quad (9)$$

Both equations yield primary proton fluxes in units of protons/cm^2-hr-Mev as a function of atmospheric depth x (g/cm^2). Two assumptions are contained in these equations. One is that the nuclear interaction cross section (which is important only for values of $\gtrsim$10 g/cm^2) has a constant value of 250 mb. This is a good assumption, as Fig. 5 shows (10 g/cm^2 = 120 Mev). The second assumption is that all primary protons enter the atmosphere vertically and hence traverse the same number of g/cm^2 of atmosphere. This is a poor assumption, and an approximate correction can be made by averaging an exponentially weighted secant to determine the effective cone of acceptance at any altitude. This then determines the effective solid angle or fraction of the fluxes calculated by Eqs. (8) and (9) to be used. This function is shown in Fig. 7.

The rad dose rate at the geomagnetic poles as a function of altitude involved multiplying Eqs. (8) and (9) by Gibson's flux-to-dose conversion function $C(E')$.[23] This function may be fit by the expression

$$C(E') = B_1 (E')^{-C_1} + B_2 (E')^{C_2} \quad (10)$$

where $C(E')$ = flux to rad dose conversion function and B_1, B_2, C_1, and C_2 are constants. In Table 4, values of the constants are given for various particles.

In order to calculate the solar flare rad dose rate, the integral of the product of Eqs. (8) and (10) was evaluated, taking the effective solid angle of Fig. 7 into account. Unfortunately, this integral cannot be evaluated analytically, and graphical techniques were used instead. The same approach was used for galactic radiation, using Eq. (9) instead of Eq. (8). This yielded the primary proton rad doses at the geomagnetic poles.

In order to take the secondary nuclear products into account (cascade and evaporation nucleons) it was necessary to evaluate expressions of the form

$$\phi_{\text{secondary}}(E'', X) = \int_0^X V\, n\sigma(E' \rightarrow E'')\phi(E', X)dx \quad (11)$$

Table 4 Parameters for fit to flux to rad dose conversion functions

Particle	B_1	C_1	B_2	C_2
Proton	4×10^{-6}	0.8	6×10^{-10}	0.85
Neutron	5×10^{-9}	0.0	1.5×10^{-10}	1.0
Alpha particle[a]	4.6×10^{-5}	0.8	7×10^{-9}	0.85

[a] Based upon fit to proton conversion function.

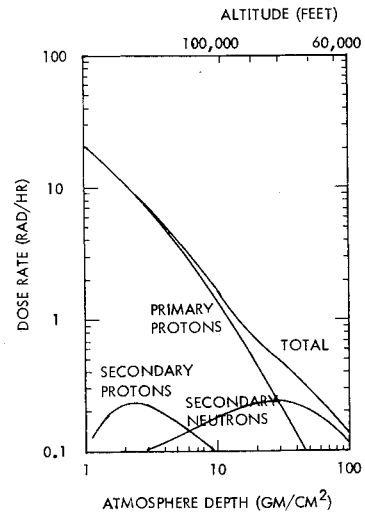

Fig. 8 Peak solar flare radiation dose rates in earth's atmosphere if no geomagnetic field.

where

V = number of one type of secondary particle per interaction (see Fig. 6)
n = density of nuclei in the atmosphere
σ = nonelastic number cross section (see Fig. 5)
ϕ = flux of primary protons [Eqs. (8) and (9)]

For cascade products, the nucleons were each assigned an energy $E'' = 0.3E'$ based upon the behavior of neighboring nuclei carbon and aluminum.[24] For evaporation products, the proton energy was taken as 8 Mev, the neutron energy as 4.5 Mev. Since the nuclear reaction products are less energetic than the primary protons, the fluxes and doses due to the secondaries will increase with atmospheric depth until an equilibrium is reached. For the secondary protons, this equilibrium will occur at atmospheric depths equal to the ranges of these particles. For secondary neutrons, the equilibrium will occur near an atmospheric depth on the order of a collision-free path. Considering galactic protons whose primary energy spectra [Eq. (4)] have maximums at $\sim$1 Bev, the cascade and evaporation secondary protons peak at $\sim$50 g/cm^2 ($\sim$70,000 ft) and 0.07 g/cm^2 ($\sim$150,000 ft), respectively, whereas the secondary neutrons peak in the neighborhood of 70 g/cm^2 ($\sim$63,000 ft), and $\sim$20 g/cm^2 ($\sim$88,000 ft), respectively.[25] For solar flare secondaries, the peaks occur at shallower atmospheric depths and will be less pronounced because of the monotonic nature of the differential energy spectrum. The calculations, which were carried out graphically, involved integrating the product

$$D(X) = \int C(E'')\phi(E'', X)dE'' \quad (12)$$

are shown in Figs. 8 and 9. Here, the rad doses due to the cascade and evaporation secondaries of a given type were lumped together to get them on one sheet of graph paper.

Although rad doses are useful in estimating radiation effects in materials, rem doses are used for estimating radiation effects in man. The rad to rem conversion function (the RBE) is a complicated factor itself, depending upon such parameters as dose rate, type and energy of particle, portion of the human body exposed, etc. One simple relationship for which there is experimental evidence is Rossi's RBE-LET relationship.[26] This relationship is shown in Fig. 10, and may be used to calculate the effective RBE values for E^{-K} spectra attenuated through shields using Eq. (6). The results are shown in Fig. 11 for solar flare and galactic charged particles.[27] For protons at all altitudes up to and including 100,000 ft, the RBE (relative biological effectiveness) may be taken as unity. RBE for neutrons was taken as equal to that of protons here. For alpha particles, the high specific ionization requires special treatment.

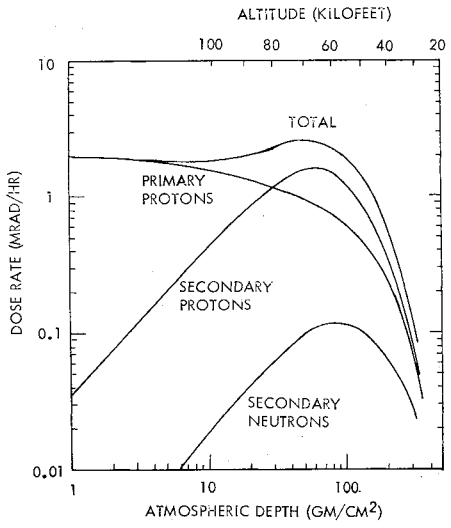

Fig. 9 Galactic radiation dose rates (quiet sun) in the earth's atmosphere if no geomagnetic field.

Up to this point in the "Shielding" section of this paper, the role of alpha particles has been neglected. Although range-energy relationships are known for alpha particles, relatively little information is available dealing with the nuclear interactions of high-energy alpha particles. The role of alpha particles is estimated by assuming that they produce four times the specific ionization of protons but only the same number of nuclear reactions, secondaries, etc. The relative populations of alpha particles to protons of the same energy in solar flare radiations has been estimated from data to be 0.8–1.[15] However, the higher ionization losses of the alpha particles result in this relative population decreasing as a function of atmosphere penetrated. Although the flux to rad dose conversion factor for alpha particles is 11.7 times (4.[1,777]) that for protons, the protons produce the majority of the rad dose at atmospheric depths 0.3 $\gtrsim$ g/cm^2. Similarly, the higher specific ionization (LET) results in a higher RBE for alpha particles, but at atmosphere depths $\gtrsim$3 g/cm^2 protons produce the majority of the rem dose. The factors by which solar flare alpha particles increase the fluxes and doses due to solar flare protons are shown in Fig. 12.[12,28] Except for the highest altitudes, these factors may be taken as unity (i.e., neglecting the solar flare alpha particles). The situation is very similar for alpha particles associated with galactic radiation. The alpha particle correction factors for galactic radiation are somewhat smaller than those shown in Fig. 12 because the relative population of alpha particles is less. For altitudes of 100,000 ft, the alpha particles may be neglected with less than a 10% error in rem dose, less than a 5% error in rad dose.

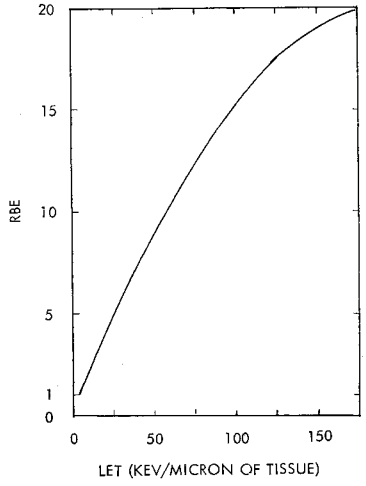

Fig. 10 The RBE-LET (relative biological effectiveness—linear energy transfer) relationship used for thiss tudy.

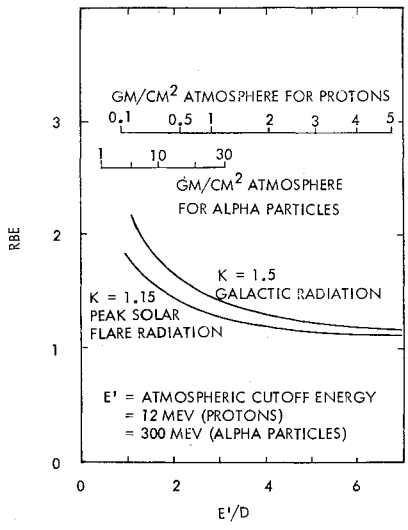

Fig. 11 RBE (relative biological effectiveness) as a function of atmospheric depth for protons and alpha particles.

So far, only the 90°-geomagnetic-latitude case has been discussed. For all other geomagnetic latitudes, there is a cutoff energy (see Fig. 4). Above this cutoff energy, the primary spectrum is considered to be unaffected. Since graphical integration was used to obtain the 90°-latitude doses, treating other latitudes only involved changing the lower limit of integration. It was assumed that the secondary particle dose contributions were proportional to the primary particle dose contributions, so the geomagnetic field was assumed to act proportionately on both.

It should be noted that the geomagnetic cutoff is decreased during periods of solar activity. However, the detailed characteristics of this decrease are not well known, and principally affect the particle fluxes at latitudes $\gtrsim$60°. In this region, the quiet sun geomagnetic cutoff energies are below the atmospheric cutoff energies so the dose rates are essentially unaffected. The results of these calculations are contained in Tables 5 and 6. Table 5 lists the rad dose rates calculated for two situations—flare, and no flare. For the no-flare situation, only the galactic radiation is present (solar minimum), whereas for the flare situation, the model flare discussed in the environment section of this paper was added. Thus the limits were calculated, since the top number is the maximum expected and the bottom number is the minimum expected. Table 6 lists the rem dose rates for the same situations.

It must be pointed out that these numbers are "point" dose rates, yielding skin and blood-forming dose rates that are somewhat lower. The effects of the aircraft, both in providing shielding and in producing secondaries, were not

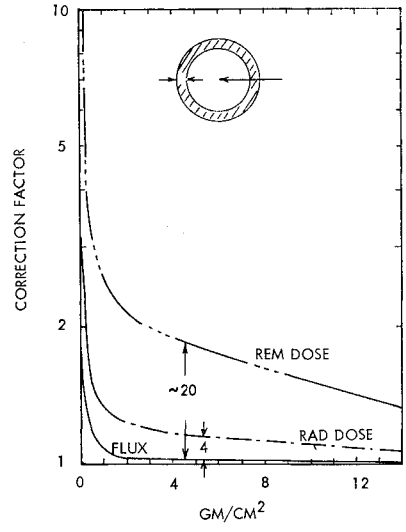

Fig. 12 Solar flare radiation correction factors to include effects of alpha particles.

Table 5 Maximum dose rates expected as function of latitude and altitude due to natural space radiation (mrad/hr)

Altitude, kft		Geomagnetic latitude, deg					
		0°	30°	45°	60°	75°	90°
10	Flare	$1.0\cdot10^{-2}$	$1.1\cdot10^{-2}$	$1.3\cdot10^{-2}$	$1.6\cdot10^{-2}$	$1.9\cdot10^{-2}$	$2.0\cdot10^{-2}$
	No flare	$1.3\cdot10^{-2}$	$1.3\cdot10^{-2}$	$1.6\cdot10^{-2}$	$2.1\cdot10^{-2}$	$2.5\cdot10^{-2}$	$2.8\cdot10^{-2}$
20	Flare	$1.3\cdot10^{-2}$	$3.0\cdot10^{-2}$	$4.5\cdot10^{-2}$	$5.5\cdot10^{-2}$	$7.5\cdot10^{-2}$	$8.0\cdot10^{-2}$
	No flare	$2.1\cdot10^{-2}$	$3.3\cdot10^{-2}$	$4.6\cdot10^{-2}$	$5.8\cdot10^{-2}$	$8.0\cdot10^{-2}$	$9.0\cdot10^{-2}$
30	Flare	$4.0\cdot10^{-2}$	$9.0\cdot10^{-2}$	$1.1\cdot10^{-1}$	$7.0\cdot10^{-2}$	$9.0\cdot10^{-2}$	$1.0\cdot10^{-1}$
	No flare	$6.3\cdot10^{-2}$	$9.0\cdot10^{-2}$	$1.3\cdot10^{-1}$	$1.7\cdot10^{-1}$	$2.0\cdot10^{-1}$	$2.1\cdot10^{-1}$
40	Flare	$6.0\cdot10^{-2}$	$2.0\cdot10^{-1}$	$2.7\cdot10^{-1}$	$3.0\cdot10^{-1}$	$5\cdot10^{-1}$	$5\cdot10^{-1}$
	No flare	$1.3\cdot10^{-1}$	$2.0\cdot10^{-1}$	$2.8\cdot10^{-1}$	$3.2\cdot10^{-1}$	$3.7\cdot10^{-1}$	$3.9\cdot10^{-1}$
50	Flare	$1.2\cdot10^{-1}$	$2.8\cdot10^{-1}$	$3.8\cdot10^{-1}$	0.8	1.8	2.5
	No flare	$1.5\cdot10^{-1}$	$3.0\cdot10^{-1}$	$4.0\cdot10^{-1}$	$5.2\cdot10^{-1}$	$6.2\cdot10^{-1}$	$6.4\cdot10^{-1}$
60	Flare	$1.3\cdot10^{-1}$	$3.0\cdot10^{-1}$	$4.7\cdot10^{-1}$	1.0	8	12
	No flare	$1.4\cdot10^{-1}$	$3.1\cdot10^{-1}$	$5.0\cdot10^{-1}$	$6.3\cdot10^{-1}$	$7.5\cdot10^{-1}$	$7.7\cdot10^{-1}$
70	Flare	$1.1\cdot10^{-1}$	$2.8\cdot10^{-1}$	$5.2\cdot10^{-1}$	2.8	40	50
	No flare	$1.3\cdot10^{-1}$	$3.0\cdot10^{-1}$	$5.5\cdot10^{-1}$	$7.1\cdot10^{-1}$	$8.3\cdot10^{-1}$	$8.7\cdot10^{-1}$
80	Flare	$8.0\cdot10^{-2}$	$2.4\cdot10^{-1}$	$5.0\cdot10^{-1}$	4.5	150	170
	No flare	$1.0\cdot10^{-1}$	$2.5\cdot10^{-1}$	$5.7\cdot10^{-1}$	$7.5\cdot10^{-1}$	$9.2\cdot10^{-1}$	$9.5\cdot10^{-1}$
90	Flare	$7.5\cdot10^{-2}$	$2.0\cdot10^{-1}$	$4.2\cdot10^{-1}$	7	480	500
	No flare	$9.0\cdot10^{-2}$	$2.2\cdot10^{-1}$	$5.6\cdot10^{-1}$	$8.0\cdot10^{-1}$	$9.5\cdot10^{-1}$	1.0
100	Flare	$7.0\cdot10^{-2}$	$1.7\cdot10^{-1}$	$3.3\cdot10^{-1}$	8	1400	1500
	No flare	$7.5\cdot10^{-2}$	$2.0\cdot10^{-1}$	$5.4\cdot10^{-1}$	$8.0\cdot10^{-1}$	1.0	1.1

considered. Since most aircraft will possess at most only a g/cm² around the crew and passengers, the aircraft will not greatly alter the calculated dose rates. The attenuation of the primary radiations by the aircraft will be partially compensated by the production of secondaries in the aircraft. For the present study, the effects of the aircraft were neglected.

Conclusions

Tables 5 and 6 contain the results of the calculations carried out in the course of this study. As expected, the largest dose rates are received at high altitudes and high latitudes during a major flare. In order to place these calculated dose rates in perspective, the NCRP (National Committee on Radiation Protection) recommends that radiation workers not be exposed to more than 5 rem/yr, or 2.5 mrem/hr for a normal 8-hr, 5-day work week. The recommended limits for the general public are a factor of 10 lower. On the other hand, it is unlikely that an aircraft would spend more than a few hours in the danger zone ($\gtrsim$60° geomagnetic latitude, $\gtrsim$50,000 ft) and that any given crew or passengers would spend more than a few hours/months on such flights. In the absence of flares, even continuous exposure is within the NCRP limits for radiation work. Therefore, a problem situation arises only when a flare occurs during such a high-altitude, high-latitude flight. In this event, the magnitude of the flare is important, since the majority of flares are only a few percent of the size of the model used for these calculations. Thus, even if it were known ahead of time that a flare would occur during a given flight, unless the magnitude of the flare were also known, it would not be possible to assess the specific hazard. Since the occurrence of flares can only be predicted statistically, and the magnitude is even less certain, the most feasible approach is to determine a course of action as the flare hazard arises. This requires knowledge of the dose rates at the position of the aircraft. The easiest method of obtaining this information is to mount a nuclear radiation detector on board. This circumvents the possibility of a communications failure because of rf blackout. The aircraft pilot can then use his judgement as to whether the radiation hazard is sufficient to require modification of his flight profile. If such modification is required, descent to a lower altitude is the most readily accomplished modification

Table 6 Maximum dose rates expected as function of latitude and altitude due to natural space radiation (mrem/hr)

Altitude, kft		Geomagnetic latitude, deg					
		0°	30°	45°	60°	75°	90°
10	Flare	$1.0\cdot10^{-2}$	$1.1\cdot10^{-2}$	$1.3\cdot10^{-2}$	$1.6\cdot10^{-2}$	$1.9\cdot10^{-2}$	$2.0\cdot10^{-2}$
	No flare	$1.3\cdot10^{-2}$	$1.3\cdot10^{-2}$	$1.6\cdot10^{-2}$	$2.1\cdot10^{-2}$	$2.5\cdot10^{-2}$	$2.8\cdot10^{-2}$
20	Flare	$1.3\cdot10^{-2}$	$3.0\cdot10^{-2}$	$4.5\cdot10^{-2}$	$5.5\cdot10^{-2}$	$7.5\cdot10^{-2}$	$8.0\cdot10^{-1}$
	No flare	$2.1\cdot10^{-2}$	$3.3\cdot10^{-2}$	$4.6\cdot10^{-2}$	$5.8\cdot10^{-2}$	$8.0\cdot10^{-2}$	$9.0\cdot10^{-1}$
30	Flare	$4.0\cdot10^{-2}$	$9.0\cdot10^{-2}$	$1.1\cdot10^{-1}$	$7.0\cdot10^{-2}$	$9.0\cdot10^{-2}$	$1.0\cdot10^{-1}$
	No flare	$6.3\cdot10^{-2}$	$9.0\cdot10^{-2}$	$1.3\cdot10^{-1}$	$1.7\cdot10^{-1}$	$2.0\cdot10^{-1}$	$2.1\cdot10^{-1}$
40	Flare	$6.0\cdot10^{-2}$	$2.0\cdot10^{-1}$	$2.7\cdot10^{-1}$	$3.0\cdot10^{-1}$	$5.0\cdot10^{-1}$	$5.0\cdot10^{-1}$
	No flare	$1.3\cdot10^{-1}$	$2.0\cdot10^{-1}$	$2.8\cdot10^{-1}$	$3.2\cdot10^{-1}$	$3.7\cdot10^{-1}$	$4.0\cdot10^{-1}$
50	Flare	$1.2\cdot10^{-1}$	$2.8\cdot10^{-1}$	$3.8\cdot10^{-1}$	0.8	1.8	2.5
	No flare	$1.5\cdot10^{-1}$	$3.0\cdot10^{-1}$	$4.0\cdot10^{-1}$	$5.2\cdot10^{-1}$	$6.2\cdot10^{-1}$	$6.5\cdot10^{-1}$
60	Flare	$1.3\cdot10^{-1}$	$3.0\cdot10^{-1}$	$4.7\cdot10^{-1}$	1.0	8	12
	No flare	$1.4\cdot10^{-1}$	$3.1\cdot10^{-1}$	$5.0\cdot10^{-1}$	$6.3\cdot10^{-1}$	$7.5\cdot10^{-1}$	$8\cdot10^{-1}$
70	Flare	$1.1\cdot10^{-1}$	$2.8\cdot10^{-1}$	$5.2\cdot10^{-1}$	3	40	50
	No flare	$1.3\cdot10^{-1}$	$3.0\cdot10^{-1}$	$5.5\cdot10^{-1}$	$7.1\cdot10^{-1}$	$8.5\cdot10^{-1}$	$9\cdot10^{-1}$
80	Flare	$8.0\cdot10^{-2}$	$2.4\cdot10^{-1}$	$5.0\cdot10^{-1}$	5	160	180
	No flare	$1.0\cdot10^{-1}$	$2.5\cdot10^{-1}$	$5.7\cdot10^{-1}$	$7.7\cdot10^{-1}$	$9.5\cdot10^{-1}$	1.0
90	Flare	$7.5\cdot10^{-2}$	$2.0\cdot10^{-1}$	$4.2\cdot10^{-1}$	8	550	600
	No flare	$9.0\cdot10^{-2}$	$2.2\cdot10^{-1}$	$5.6\cdot10^{-1}$	$8.5\cdot10^{-1}$	1.0	1.2
100	Flare	$7.0\cdot10^{-2}$	$1.7\cdot10^{-1}$	$3.4\cdot10^{-1}$	10	2000	2500
	No flare	$7.5\cdot10^{-2}$	$2.0\cdot10^{-1}$	$5.5\cdot10^{-1}$	$9.0\cdot10^{-1}$	1.1	1.2

that will reduce the hazard. In no event should it be necessary to descend much below 50,000 ft because of the occurrence of a solar flare. By observing the nuclear radiation detector, the pilot could determine when it was desirable to ascend after the hazard had passed.

It appears that there will be no radiation damage effects to aircraft components as a result of nuclear space radiation. Even the semiconductor electronic components have damage thresholds that will give them operating lifetimes of several years at 100,000 ft and 90° latitude. Structure and other aircraft materials will be unaffected by space radiation for the conditions considered.

References

[1] Schaefer, H. J., "Depth of penetration of solar protons into the atmosphere and related radiation exposure in the supersonic transport," Aerospace Med. **34,** 1–4 (1963).

[2] Dye, D. L. and Sheldon, W. R., "Some radiation problems in the supersonic environment," The Boeing Company, Rept. D2-90391 (1963).

[3] Shen, S. P., "Space radiation and the supersonic transport," General Electric Company, Rept. R64SD1 (1964).

[4] Mohler, S. R., "Ionizing radiation and the SST," Astronautics and Aeronautics **2,** 60–68 (1964).

[5] Foelsche, T., "The ionizing radiations in supersonic transport flights," *Proceedings of the Second Symposium on Protection against Radiation Hazards in Space,* NASA SP-71 (1964), pp. 287–300.

[6] Nold, M. M., Adams, D. A., and Supko, P. R., "A critique of the biological significance of the supersonic transport radiation environment," Aerospace Med. **37,** 829–833 (1966).

[7] Forbush, S. E., "The unusual cosmic ray increase possibly due to charged particles from the sun," Phys. Rev. **70,** 771 (1946).

[8] Webber, W. R., "An evaluation of the radiation hazard due to solar particle events," The Boeing Company, Rept. D2-90469 (1963).

[9] McDonald, F. B., "Solar proton manual," NASA TR-R-169 (1963).

[10] Lewis, L. R., Brown, G.M., Gabler, J., and Magee, R. M, "Solar flare radiation survey," Air Force Doc. RTD-TDR-63-3044 (1963).

[11] Glasstone, S., *Sourcebook on Atomic Energy* (D. Van Nostrand Company Inc., New York, 1958), 2nd ed., Chap. XVIII, pp. 554–572.

[12] Saylor, W. P., Winer, D. E., Eiwen, C. J., and Carriker, A. W., "Space radiation guide," Air Force Doc. AMRL-TDR-62-86 (1962).

[13] Haffner, J. W., "Shielding analysis of 1956–1961 solar proton event data," North American Aviation Inc., Rept. SID 64-1295 (1964).

[14] Haffner, J. W., "An attenuation kernal for the bailey model event," Trans. Am. Nucl. Soc. **7,** 16 (1964).

[15] Haffner, J. W., "The role of alpha particles in shielding against solar event radiation," North American Aviation Inc., Rept. SID 64-1297 (1964).

[16] Haffner, J. W., "The role of galactic protons in shielding against space radiation," North American Aviation Inc., Rept. SID 64-2036 (1964).

[17] Williams, R. W., "Cosmic rays and high-energy phenomena," *Fundamental Formulas of Physics* (Dover Publications Inc., New York, 1960), Chap. 23, p. 561.

[18] Fano, U., "Penetration of protons, alpha particles, and mesons," Ann. Rev. Nucl. Sci. **13,** 1–66 (1963).

[19] Sternheimer, R. M., "Range-energy relations for protons in Be, C, Al, Cu, Pb, and air," Phys. Rev. **115,** 137–142 (1959).

[20] Alter, H., "Basic microscopic data for space shielding analysis," North American Aviation Inc., Memo AI-8853, Vol. 1 (1963).

[21] Bertini, H. W., "A literature survey of non-elastic reactions for nucleons and pions incident on complex nuclei at energies between 20 mev and 33 gev," Oak Ridge National Lab., Rept. ORNL-3455 (1963).

[22] Bertini, H. W., "Parametric study of calculated cascade and evaporation reactions for 25-400 mev nucleons incident on complex nuclei," Oak Ridge National Lab., Rept. ORNL-3499, No. 2, pp. 31–53 (1963).

[23] Gibson, W. A., "Energy removed from primary proton and neutron beams by tissue," Oak Ridge National Lab., Rept. ORNL-3260 (1962).

[24] Keller, J. W., "A study of shielding requirements for manned space missions," Convair, Rept. FZK-124 (1960).

[25] Peters, B., "Cosmic rays," *Handbook of Physics* (McGraw-Hill Book Company Inc., New York, 1958), 1st ed., Chap. 12, pp. 9-201–9-244.

[26] Lindenbaum, S. J., "Shielding of high energy accelerators," Ann. Rev. of Nucl. Sci. **11,** 213–258 (1961).

[27] Haffner, J. W., "RBE of protons and alpha particles," *Proceedings of the Second Symposium on Protection against Radiation Hazards in Space,* NASA SP-71 (1964), pp. 513–525.

[28] Madey, R. and Stephenson, T. E., "Quality factors for degraded proton spectra," *Proceedings of the Second Symposium on Protection against Radiation Hazards in Space,* NASA SP-71 (1964), pp. 229–234.